C S

Inositol-1,4,5-trisphosphate Induces Responses in Receptor Neurons in Rat Vomeronasal Sensory Slices

Kouhei Inamura, Makoto Kashiwayanagi and Kenzo Kurihara

Faculty of Pharmaceutical Sciences, Hokkaido University, Sapporo 060, Japan

Correspondence to be sent to: Dr Makoto Kashiwayanagi, Faculty of Pharmaceutical Sciences, Hokkaido University, Sapporo 060, Japan

Abstract

Using the whole-cell mode of the patch-clamp technique, we recorded action potentials, voltage-activated cationic currents and putative second messenger-activated currents in receptor neurons in the vomeronasal sensory epithelium of female rats. The resting membrane potential and input resistance were –45.5 ± 2.5 mV (mean ± SEM, n = 39) and 1.5 ± 0.2 GΩ (mean ± SEM, n = 37). Current injection of 1–3 pA induced overshooting action potentials. The firing frequency increased with increasing current injections linearly from 1 to 10 pA and reached a plateau at 30 pA, suggesting that rat vomeronasal receptor neurons sensitively elicit action potentials in response to a small receptor potential. Under voltage clamp, voltage-dependent Na^+ inward current, inward Ca^{2+} current, sustained outward K^+ current and Ca^{2+}-activated K^+-current were identified. Dialysis of D-inositol-1,4,5-trisphosphate (D-IP_3) induced inward currents with an increase in membrane conductance in ~54% of the cells and inward current fluctuations in 15% of the cells. L-IP_3 also induced inward currents and current fluctuations in 53 and 13% of the cells respectively. The mean amplitude of inward currents induced by 100 μM D-IP_3 and L-IP_3 were 84.6 ± 14.0 pA (SEM, n = 82) and 66.1 ± 9.4 pA (SEM, n = 100) respectively. The IP_3-induced responses were blocked by elimination of Na^+ and Ca^{2+} in the external solution or application of 10 μM ruthenium red. The present study suggested that IP_3-mediated transduction pathways exist in rat vomeronasal receptor neurons. **Chem. Senses 22: 93–103, 1997.**

Introduction

The olfactory organ and the vomeronasal organ exist in many vertebrates as olfactory systems. The latter organ relates social and sexual behavior and is preferentially sensitive to pheromones (Powers and Winans, 1975; Wysocki *et al.*, 1980; Rajendren and Dominic, 1985; Halpern, 1987; Wysocki and Meredith, 1987; Jiang *et al.*, 1990; Sipos *et al.*, 1995). Regulation of gonadal functions such as effects of urine on the timing of estrous cycles (Johns *et al.*, 1978) and the excretion of the puberty-delay chemosignal (Lepri *et al.*, 1985) were well established in rodent vomeronasal organ. Urinary compounds of low volatility, which do not reach the olfactory epithelium, may stimulate the vomeronasal system and provide information that is normally not provided by gustation or olfaction (Wysocki *et al.*, 1980).

The receptor mechanisms of the vomeronasal organ have been investigated mainly in reptiles and amphibians. The functional adenylyl cyclase was shown biochemically in

reptile vomeronasal sensory epithelia; application of forskolin, guanosine triphosphate (GTP) and GTPγS to the membrane preparations of the snake and the turtle vomeronasal epithelia induced cAMP accumulation (Luo *et al.*, 1994; Okamoto *et al.*, 1996). In the turtle vomeronasal receptor neuron (Taniguchi *et al.*, 1996b), cAMP dialyzed from the patch pipette induced an inward current in a similar dose-dependent manner to that in the turtle olfactory neuron (Kashiwayanagi and Kurihara, 1995), suggesting that the vomeronasal receptor neuron and the olfactory receptor neuron possess similar cyclic nucleotide-mediated transduction pathway in the turtle. Application of forskolin to the turtle vomeronasal sensory epithelium induced an increase in impulse frequency in the vomeronasal receptor neuron and increased activity of brain waves at the turtle accessory olfactory bulb (Taniguchi *et al.*, 1996a,b). These results suggest that depolarization mediated via cyclic nucleotide-gated ion channels generates action potentials in the turtle vomeronasal receptor neuron.

Mammalian vomeronasal receptor neurons possess distinct cyclic nucleotide-mediated transduction molecules from olfactory receptor neurons (Berghard and Buck, 1996; Berghard *et al.*, 1996). In the mouse vomeronasal epithelium, $G_{i\alpha}$, $G_{o\alpha}$ proteins and mRNAs encoding adenylyl cyclase type II and cyclic nucleotide-gated channel (rOCNC2), which did not form functional channels alone (Bradley *et al.*, 1994; Liman and Buck, 1994), were shown to be localized (Halpern *et al.*, 1995; Jia and Halpern, 1996; Berghard and Buck, 1996; Berghard *et al.*, 1996). Dialysis of cAMP into mouse vomeronasal receptor neurons did not induce inward currents, suggesting that cyclic nucleotide-gated channels may not mediate transduction in mouse vomeronasal receptor neurons (Liman and Corey, 1996).

In the garter snake, ES20, a chemoattractant extracted from its prey (Jiang *et al.*, 1990), induced inositol-1,4,5-trisphosphate (IP_3) accumulation (Luo *et al.*, 1994). Dialysis of IP_3 into the turtle vomeronasal receptor neurons induced inward currents (Taniguchi *et al.*, 1995). These results suggest that pheromonal information is mediated via the IP_3-dependent pathway in the vomeronasal receptor neurons. In the present study, we studied IP_3-activated currents in the rat vomeronasal receptor neuron to obtain information about the transduction mechanism of the mammalian vomeronasal receptor neurons under whole-cell voltage-clamp conditions. The results obtained suggested that the IP_3-mediated transduction pathway exists in rat vomeronasal receptor neurons. In addition, we examined the characteristics of voltage-dependent cation channels of the neuron under whole-cell current-clamp and voltage-clamp conditions. Injections of 1–40 pA into the receptor neurons elicited steady trains of action potentials in a dose-dependent manner, indicating that voltage sensitivity of rat vomeronasal receptor neurons is very high.

Materials and methods

Slice preparation of rat vomeronasal sensory epithelium

Female Wistar rats, weighing 160–250 g, were obtained from a commercial supplier (Sankyo Laboratory Co. Ltd, Sapporo, Japan). The methods were essentially similar to those described in the previous paper (Taniguchi *et al.*, 1996b). Vomeronasal epithelium was quickly removed from the decapitated rats. The epithelia were cut into slices ~120 μm thick with a vibrating slicer (DTK-1000, DTK, Kyoto, Japan) in normal Tyrode solution at 0°C and stored at 4°C. Epithelial slices were fixed on the glass at the bottom of a recording chamber, permitting access to cells on the surface of the slice by the patch pipette. The preparations were viewed under an upright microscope (Optiphot model, Nikon, Tokyo, Japan) using a ×40 water immersion lens.

Data recording and analysis

The conventional whole-cell patch-clamp method was used to measure transmembrane currents (Hamill *et al.*, 1981). Patch pipettes with resistances of 5–10 MΩ were made from borosilicate glass capillaries with inner filament (GD-1.5, Narishige Co., Tokyo, Japan) using a two-stage electrode puller (PP853, Narishige) and then heat-polished. Giga-ohm seals were obtained by applying negative pressure (–30 to –100 cm H_2O). The whole-cell configuration was attained by application of additional negative pressure. Membrane currents (holding potential, –70 mV) and voltages were recorded in the whole-cell configuration. Data were recorded continuously using an EPC-7 patch clamp amplifier (List, Darmstadt, Germany) and stored on video cassette via a digital audio processor (PCM-501, Sony, Tokyo, Japan). All recordings were performed at room temperature. Analysis was carried out on a personal computer using pCLAMP software (Axon Instruments, Foster City, USA). All values are given as mean ± SEM.

Lucifer Yellow dialysis

Lucifer Yellow CH was dialyzed intracellularly by using the patch pipettes filled with 1% Lucifer Yellow solution as described previously (Taniguchi *et al.*, 1996b). After the measurement of voltage-activated currents, the pipettes were pulled back from the surface of the cells. Then, the specimens were transferred to the stage of a fluorescent microscope (Optiphot) and observations were made under fluorescent illumination.

Solutions

Extracellular Tyrode solution consisted of (in mM): 145 NaCl, 2.5 KCl, 2 $CaCl_2$, 10 glucose, 10 HEPES-NaOH (pH 7.4). Patch pipettes were usually filled with a normal internal solution (in mM): 140 KCl, 2.5 $MgCl_2$, 0.5 ATP, 0.5 EGTA, 10 HEPES–KOH (pH 7.2). Further details of the solutions are shown in the individual figure legends. Lucifer Yellow was dissolved in the internal solution at a concentration of 1%.

Chemicals

Tetrodotoxin (TTX) and Lucifer Yellow CH were obtained from Sankyo (Tokyo, Japan) and Aldrich Chemical Co. (Milwaukee, USA) respectively. D- and L-IP_3 were obtained from Sigma Chemical Company (St Louis, MO, USA).All chemicals used were of the highest grade available.

Results

Cell morphology

Figure 1 shows light (A) and fluorescent (B) micrographs of the rat vomeronasal sensory epithelium. The vomeronasal receptor neurons in the vomeronasal sensory epithelium have a similar structure to that of the turtle as reported previously (Taniguchi *et al.*, 1996b). Cell bodies are elliptical with dimensions in the order of 20 × 13 μm. Cells have dendritic processes which reach to the surface of the epithelium. Microvillus structures are not shown in the figure but were identified.

Cell-attached recording

Before the breakthrough, spontaneous action potential patch currents were observed at cell-attached mode in at least 54 cells (Figure 1C). The frequency of action potentials shown in the figure was 10 Hz. Action potentials were induced by depolarization of cell-attached patches in ~63% of cells (Figure 1D).

Current-clamp recordings

The initial studies of the whole-cell clamp technique were made using the current-clamp mode. With K^+ and Na^+ as the main internal and external membrane-permeable cations respectively, the mean resting membrane potential for these cells was –45.5 ± 2.5 mV (n = 39), similar to the value measured in the turtle vomeronasal receptor neuron (Taniguchi *et al.*, 1996b). Injection of current (1–3 pA) elicited action potentials from conditioning voltage at –60 mV (Figure 2A). The threshold for action potential generation in these cells was commonly between –35 and –55 mV. A large current injection generated brief trains of action potentials (Figure 2B). Impulse trains typically consisted of up to 20 spikes. The firing frequency increased with increasing current injections linearly from 1 to 10 pA and reached a plateau at 30 pA (Figure 2C). The action potential latency was reduced with increasing amplitude of current injection. The current-induced spike was shown to be sensitive to 10 μM TTX (Figure 2D,E), suggesting that a voltage-sensitive Na^+ current was involved in its generation.

Voltage response to injected current

Voltage-clamp recordings confirm that the current responsible for the rising phase of the current-induced action potential was carried by Na^+. Figure 2(F) shows the two major currents elicited by depolarizing steps of voltage from a holding potential of –70 mV. A transient inward current appeared at –40 mV and became larger with more depolarizing steps reaching up to –2.1 nA at –20 mV. With further depolarization, this current diminished but the outward current was seen following the rapid inward current. The current–voltage curves taken at the peak of the inward current and the outward current are shown in Figure 2(G). The input resistance was determined by measuring the response to a step in command potential from –100 to –60 mV, a region where no voltage-gated currents are present. The measured mean input resistance ranged from 0.3 to 4.0 GΩ (1.5 ± 0.2 GΩ, n = 37).

To examine the transient inward currents, internal KCl was substituted with CsCl. Figure 3(A) shows a transient inward current elicited by voltage steps between –60 and –10 mV from a 200 ms prepulse of –160 mV. At –40 mV, it reached a peak magnitude of ~3400 pA within 3 ms. The

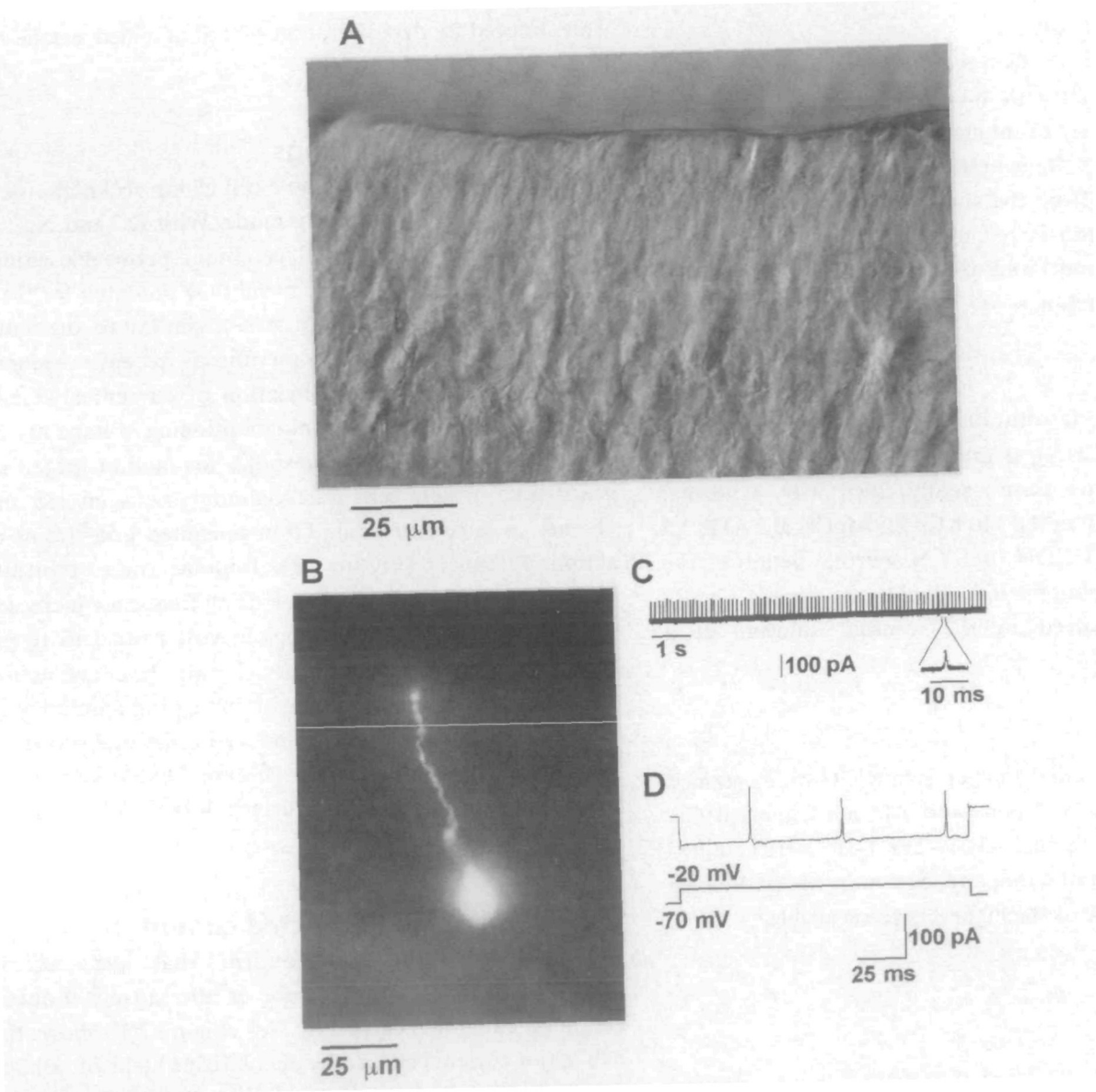

Figure 1 Rat vomeronasal receptor neurons in the sensory epithelium. (**A**) Phase-contrast photomicrograph of a slice of a vomeronasal epithelium. (**B**) A vomeronasal receptor neuron dialyzed with 1% Lucifer Yellow. The knob-like structure, long dendrite and soma are visible. Voltage-activated currents were observed in the neuron (*data not shown*). (**C**) Spontaneous action potentials recorded at on-cell mode. Imposed trace indicates a part of the same recording shown in upper trace in an expanded time scale. (**D**) The response of the cell to sustained current injection.

peak magnitude varied from –920 to –3400 and the mean magnitude was 2148 ± 279 pA (n = 8) at –37 mV. The activation threshold was near –50 mV. The voltage-dependence of steady-state inactivation was determined by applying a 50 ms depolarizing test pulse to –40 mV preceded by a 200 ms conditioning pulse to voltages from –130 mV to –40 mV in 10 mV steps (Figure 3C). The resulting data were fitted with a Boltzmann distribution and subsequent fits were used to determine the potential where inactivation was half-maximal (Figure 3D). The current was completely inactivated by conditioning potentials >–50 mV. In a total of eight cells analyzed, the inactivation midpoint was –82.8 ± 4.4 mV, ranging from –110 to –67 mV. Replacing Na^+ with choline in the external solution reversibly and completely abolished the transient inward current in 10 out of 11 cells (Figure 3E). Although a small TTX-insensitive inward current was observed in 2 out of 13 cells (Figure 3F), addition of 10 μM TTX to external solution also completely inhibited this current in most cells (data not shown). These results suggest that the current is probably carried by Na^+.

A voltage-dependent inward current was also observed in the vomeronasal receptor neuron even in the presence of 10 μM TTX (Figure 3F). This current was ~80 pA and blocked by elimination of Ca^{2+} in the external solution. To

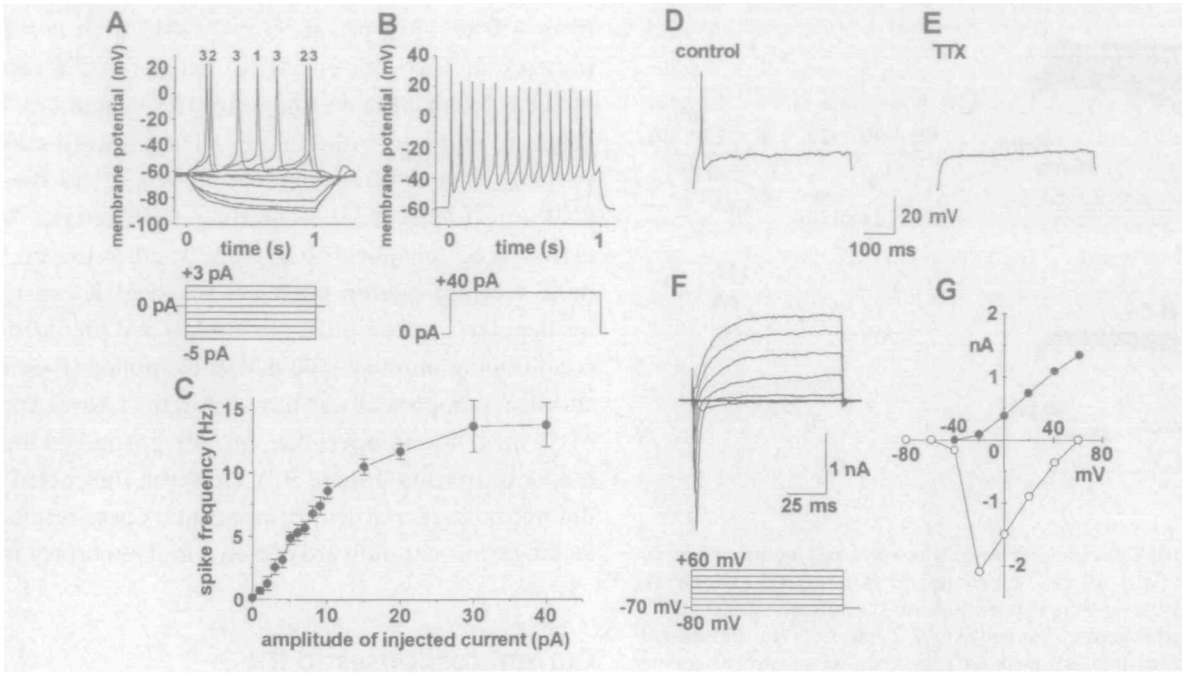

Figure 2 Current- and voltage-clamp recordings from rat vomeronasal receptor neurons. Current-clamp recording showing the voltage responses to positive current injections from conditioning potential at –60 mV (**A**). Above a certain threshold, action potential spikes were observed. The number above action potentials indicates amplitude of currents injected. Repetitive action potentials evoked by a large current step (40 pA) at –50 mV (**B**). These traces (A,B) were recorded from the same cell. (**C**) Spike frequency of vomeronasal receptor neurons as a function of current injection for seven cells that fired repetitively. (**D**) An action potential recorded in response to a positive current pulse (40 pA) from the conditioning potential (–55 mV). (**E**) This action potential response was blocked by 10 μM TTX. (**F**) The currents seen under voltage-clamp in response to negative and positive voltage pulses. (**G**) Current–voltage relations Peak of the transient inward current (open circle) and the outward current (closed circle).

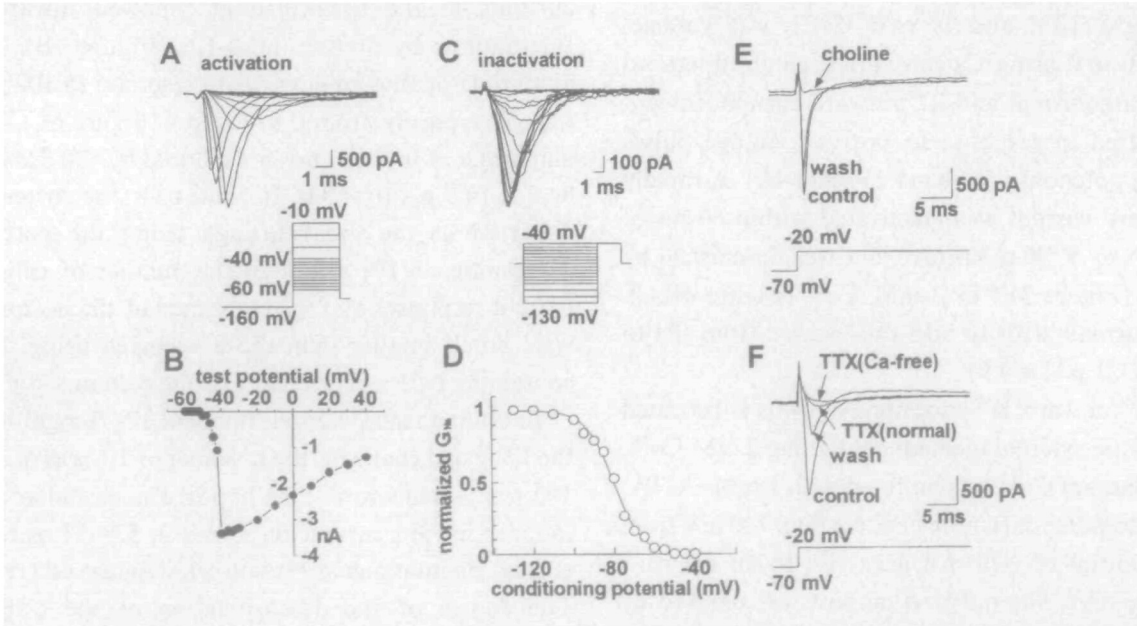

Figure 3 Isolated Na^+ currents from rat vomeronasal neurons. (**A**) The Na^+ current responses to positive and negative voltage pulses to the membrane potentials from a prepulse potential of –160 mV. (**B**) Plot of transient peak Na^+ current against membrane potential. (**C**) The Na^+ current responses to a voltage pulse to –40 mV from prepulse potentials between –130 and –40 mV. (**D**) plot of normalized peak current amplitude against prepulse potential. The voltage-activated Na^+ current is blocked following the substitution of Na^+ with choline in the external solution (**E**) or addition of 10 μM TTX to the external solution (**F**). Elimination of Ca^{2+} in the external solution by addition 1 mM EGTA completely blocks the TTX-insensitive inward current (**F**). Internal solution composition (in mM): 140 CsCl, 2.5 $MgCl_2$, 0.5 ATP, 0.5 EGTA, 10 HEPES–NaOH (pH 7.2) External EGTA solution composition (in mM): 145 NaCl, 2.5 KCl, 1 EGTA, 10 glucose, 10 HEPES–NaOH (pH 7.4).

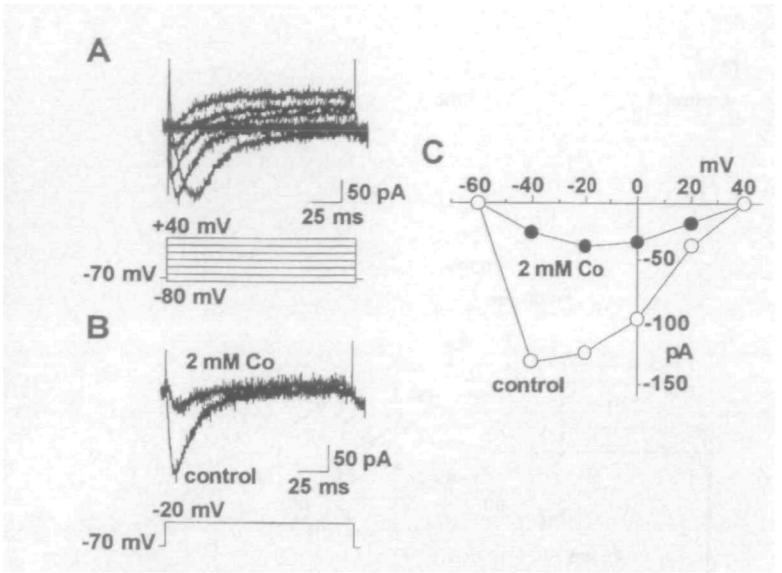

Figure 4 Isolated Ca^{2+} currents from rat vomeronasal receptor neurons, and the effect of Co^{2+}. (**A**) Ca^{2+} current responses to negative and positive voltage pulses to the membrane potentials. (**B**) The voltage-activated Ca^{2+} current is blocked following the addition of 2 mM Co^{2+} to the external solution. (**C**) Plot of transient peak Ca^{2+} current and against membrane potential in Tyrode solution (open circle) and that containing 2 mM Co^{2+} (closed circle). Internal solution contained (in mM): 140 CsCl, 2.5 $MgCl_2$, 0.5 ATP, 0.5 EGTA, 10 HEPES–NaOH (pH 7.2). External solution contained (in mM): 125 choline, 15 TEA, 10 $CaCl_2$, 0.001 TTX, 10 glucose, 10 HEPES–CsOH (pH 7.4).

confirm the currents carried through Ca^{2+} channels, the vomeronasal receptor neuron in external solution containing 1 μM TTX and 10 mM $CaCl_2$ was voltage-clamped at –70 mV using Cs-containing patch pipette to block Na^+ inward current and K^+ outward current. Inward currents appeared in response to positive voltage pulses from a holding potential of –70 mV (Figure 4A). A rapidly activating inward current was inactivated within 60 ms of pulse onset; it was TTX insensitive, but was diminished by 1 mM EGTA (Figure 3F) or 2 mM Co^{2+} (Figure 4B,C). Peak inward currents with 10 mM Ca^{2+} varied from –21 to –622 pA (171 ± 21 pA; n = 9).

To study the outward K^+ currents, Na^+ was substituted with choline in the external medium containing 2 mM Co^{2+}, and any contaminant Ca^{2+} was buffered with 1 mM EGTA. Voltage pulses to potentials more positive than –40 mV from a holding potential of –70 mV gave rise to an outward current (Figure 5A). The outward current was blocked by addition of 25 mM TEA to the external solution (Figure 5B) in eight out of eight cells. The outward currents reversibly appeared after elimination of TEA in the external solution (Figure 5C). A plot of the current at the peak versus membrane potential (Figure 5D) revealed a current that increased with potential up to a membrane potential as high as 100 mV. The amplitude of this end K^+ current varied from 430 to 2735 pA at 60 mV (1412 ± 5; n = 92). The presence of Ca^{2+}-dependent K^+ current in the neuron was studied by measuring the outward current in external solution with and without Ca^{2+}. The outward current was partially attenuated by elimination of Ca^{2+} in the external solution (Figure 5E), suggesting the presence of Ca^{2+}-activated K^+ channel. To explore whether the rat vomeronasal receptor neuron possesses transient K^+ currents, 150 ms depolarizing test pulses to 40~100 mV preceded by a 2 s conditioning pulse at –100 mV were applied (Figure 5F). A transient component was not seen in the figure. Application of 2 mM 4-aminopyridine (4-AP) partially blocked the outward currents (Figure 5G). However, subtracted currents did not possess transient components. These results suggest lacking transient outward currents in the receptor neuron.

Current responses to IP_3

To study the effects of a putative second messenger on the rat vomeronasal receptor neuron, 100 μM D-IP_3 was dialyzed from the patch pipette into the neuron. On the breaking of the patch, D-IP_3 induced inward currents in 44 out of 82 cells and the current was then desensitized in 38 cells (Figure 6A). Twelve cells, which did not possess inward currents at the breakthrough, showed inward current fluctuations by dialysis of D-IP_3 (Figure 6B). The peak amplitude of inward currents in response to 100 μM D-IP_3 ranged, typically, from 0 to 628 pA (Figure 6C). The mean amplitude of inward currents induced by 100 μM D-IP_3 was 84.6 ± 14.0 pA (n = 82). In some cells, the current changes occurred at the breakthrough using the patch pipette containing no IP_3 although the number of cells showing current responses and the amplitude of the inward currents were much smaller than those occurred using the pipette containing D-IP_3, respectively (white columns in Figure 6C).

To evaluate the stereoselectivity of IP_3 recognition sites of the IP_3-gated channels, the L-isomer of IP_3 was dialyzed into 100 receptor neurons. One hundred micromolar L-IP_3 also induced inward current responses in 53% (Figure 6D) and current fluctuations in 13% of cells (Figure 6E) respectively. The degree of the desensitization of the L-IP_3-induced current was lower than that of the D-IP_3-induced current; L-IP_3-induced current was completely desensitized only in 24 out of 53 cells. The peak amplitude of inward currents induced by L-IP_3 ranged, typically, from 0 to 400 pA (Figure 6F). The mean amplitude of inward currents induced by L-IP_3 (66.1 ± 9.4 pA) was slightly smaller than that by D-IP_3

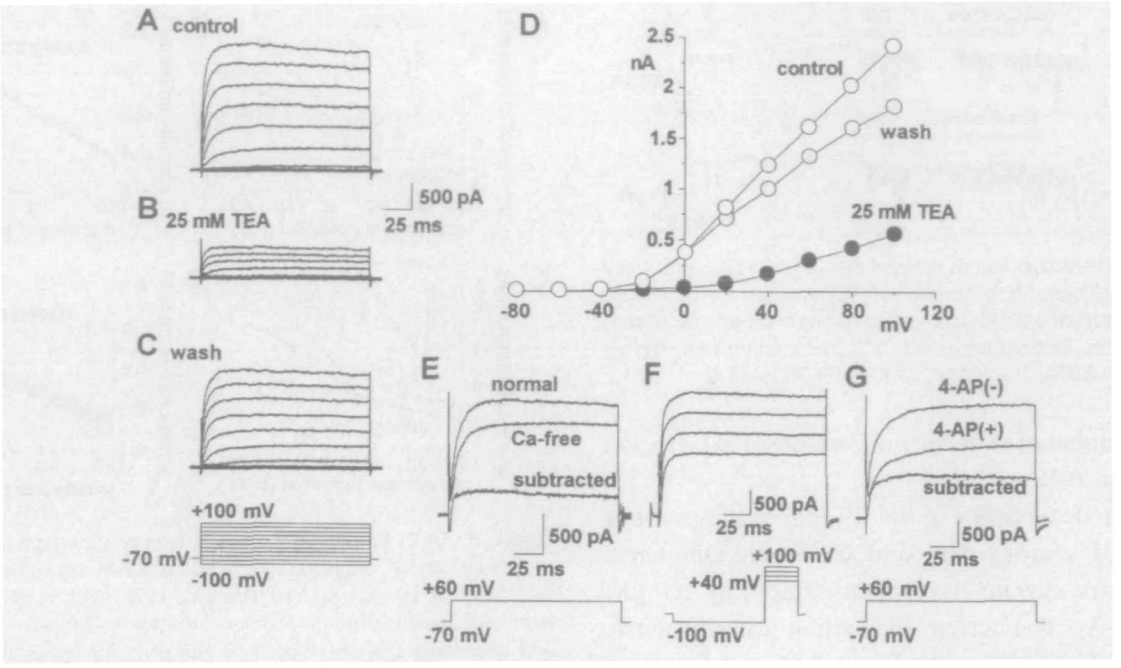

Figure 5 Isolated K^+ currents in rat vomeronasal receptor neurons, and the effect of application of TEA and 4-AP and elimination of Ca^{2+}. (**A**) The K^+ current responses to positive voltage pulses from a holding potential of –70 mV. This current was reversibly blocked by 25 mM TEA (**B**,**C**). (**D**) Current–voltage relationship for the sustained outward current for the neuron shown in (A–C), measured at the peak of the current. External solution contained (in mM): 147 choline, 1 EGTA, 2 $CoCl_2$, 0.001 TTX, 10 glucose, 10 HEPES–KOH (pH 7.4). (**E**) The outward K^+ current is partially attenuated by elimination of Ca^{2+} from the external solution. Ca^{2+}-free solution contained (in mM): 147 choline, 1 EGTA, 0.001 TTX, 10 glucose, 10 HEPES–KOH (pH 7.4). Normal, Tyrode solution. (**F**) the K^+ current responses to positive voltage pulses from a prepulse of –100 mV. (**G**) The outward K^+ current is partially blocked following the addition of 2 mM 4-AP to the external solution.

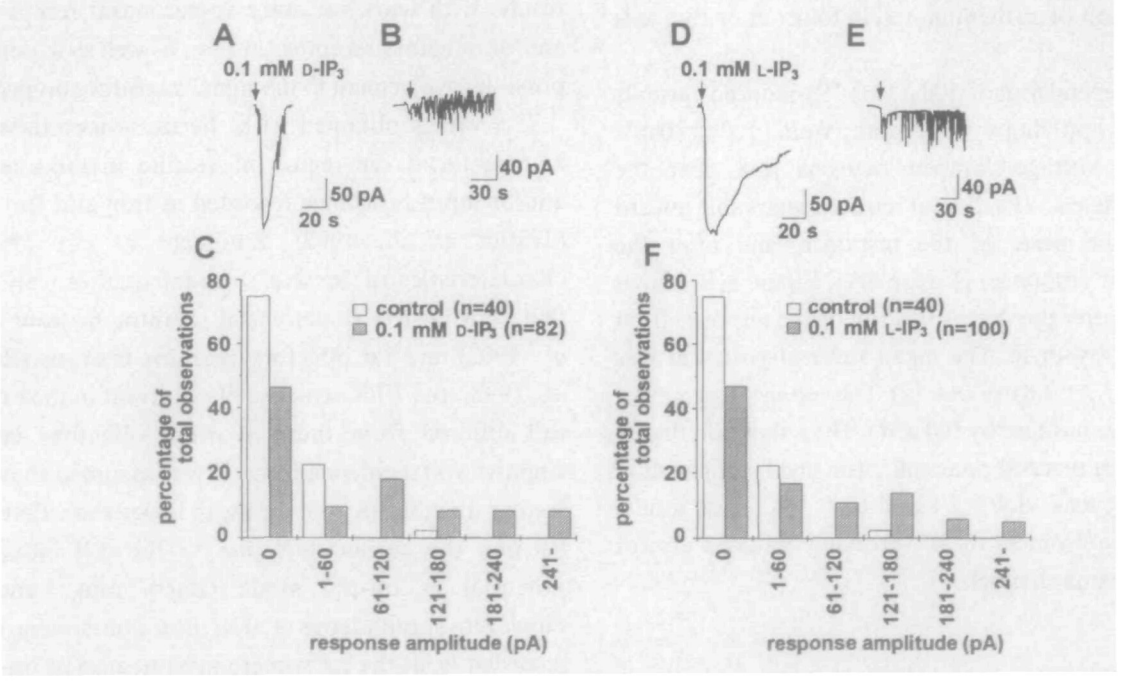

Figure 6 IP_3-induced inward currents recorded from rat vomeronasal receptor neurons under the whole-cell voltage-clamp condition. (**A**,**B**) Membrane currents at the breakthrough measured with the pipette containing 100 μM D-IP_3 under voltage-clamp with a holding potential at –70 mV. (**C**) Distribution of the peak amplitude of inward currents induced by intracellularly applied 100 μM D-IP_3 in 82 cells (shadowed column) and by a normal internal solution in 40 cells. (**D**,**E**) membrane currents at the breakthrough measured with the pipette containing 100 μM L-IP_3 under voltage-clamp with a holding potential at –70 mV. (**F**) Distribution of the peak amplitude of inward currents induced by intracellularly applied 100 μM L-IP_3 in 100 cells (shadowed column) and by a normal internal solution in 40 cells.

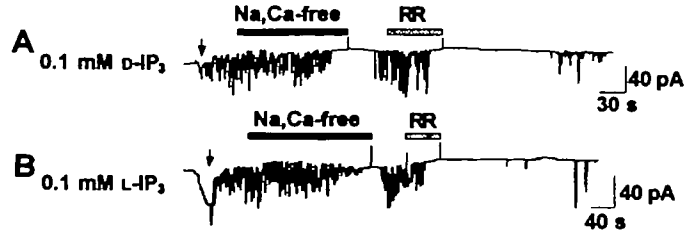

Figure 7 (A,B) current fluctuations induced by 100 μM D-IP$_3$ and 100 μM L-IP$_3$ were reversibly blocked by elimination of Na^+ and Ca^{2+} in the external solution or 10 μM ruthenium red (RR) applied during a period indicated by bars upper the traces. External Na^+- and Ca^{2+}-free solution contained (in mM): 150 choline, 1 EGTA, 10 glucose, 10 HEPES–KOH (pH 7.4).

although the number of cells showing responses to L-IP$_3$ was similar to that to D-IP$_3$.

To test the ion dependence of the IP$_3$-induced response in rat vomeronasal neurons, Na^+ and Ca^{2+} were eliminated during the inward current fluctuation induced by 100 μM D-IP$_3$ (Figure 7A). The current fluctuation was completely blocked by the elimination of Na^+ and Ca^{2+} in three out of three cells. When the outer Na^+ and Ca^{2+} were replenished, the current fluctuation appeared. The current fluctuation induced by D-IP$_3$ was completely inhibited by 10 μM ruthenium red in five out of five cells (Figure 7A). The current fluctuation induced by 100 μM L-IP$_3$ was also attenuated by elimination of Na^+ and Ca^{2+} in five out of five cells or application of ruthenium red in four out of five cells (Figure 7B).

The voltage-dependence of 100 μM D-IP$_3$-induced currents was examined by applying a voltage ramp from –120 to 80 mV (500 mV/s) to voltage-clamped neurons just after the breakthrough where D-IP3 did not induce remarkable inward current, near the peak of the response, and after the desensitization of responses (Figure 8A). Figure 8(B) shows subtraction one after the desensitization of the response from one during the response. The mean reversal potential was estimated to be -7.2 ± 3.8 mV ($n = 12$). The voltage-dependence of inward currents induced by 100 μM L-IP3 is shown in Figure 8(C,D). The mean reversal potential estimated by application of 100 μM L-IP$_3$ was -3.4 ± 2.8 mV ($n = 11$). These results suggest that stereoisomers of IP$_3$ probably induced inward currents via the same channel.

Discussion

In this study, we have used the whole-cell voltage-clamp technique to study the electrophysiological properties of receptor neurons in the rat vomeronasal sensory epithelium.

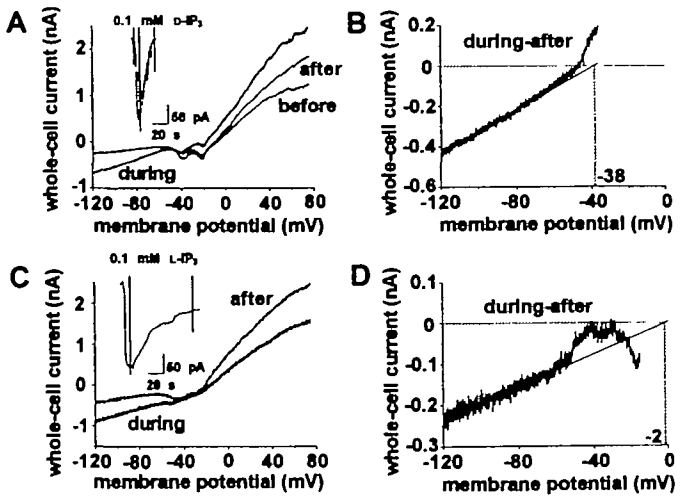

Figure 8 (A,C) Whole-cell current-voltage relationships for the current evoked by internal 100 μM D-IP$_3$ and 100 μM L-IP$_3$ respectively The current was measured by applying a voltage ramp (500 mV/s) from –120 to 80 mV before, during and after the response induced by 100 μM D-IP$_3$ and during and after the responses induced by 100 μM L-IP$_3$ respectively. The insets show the records of the IP$_3$-induced responses of these cells under whole-cell voltage-clamp condition at –70 mV. (B,D) D-IP$_3$-induced current and L-IP$_3$-induced current were obtained by subtracting currents after the response from during a sustained response shown in the insets. The reversal potentials were –38 mV in (B) and –2 mV in (D) respectively.

We have recorded responses to IP$_3$ and have separated the voltage-gated currents. It is of interest to compare these results with work on other vomeronasal receptor neurons and/or olfactory receptor neurons, as well as to consider their possible involvement in the signal transduction process.

The values obtained with the rat vomeronasal receptor neuron lie in the region of resting membrane potential and/or input resistance recorded in frog and turtle neurons (Trotier *et al.*, 1993; Taniguchi *et al.*, 1996b). The characteristics of the Na^+ current qualitatively resembles that seen in frog vomeronasal receptor neurons (Trotier *et al.*, 1993) and rat olfactory receptor neurons (Rajendra *et al.*, 1992); the TTX-sensitive Na^+ current in the rat olfactory cell differed from them in other olfactory cells in the negative voltage-dependence. It was assumed that the actual resting membrane potential was lower than that measured because the current injection to the cell induced action potential at on-cell mode (Barry and Lynch, 1991). However, spontaneous action potentials were sometimes recorded from the rat vomeronasal neuron at on-cell mode, suggesting that voltage-dependent Na^+ channels in some vomeronasal neurons may be activated at the resting membrane potential.

Action potentials were evoked by only a small currents injected in the rat vomeronasal receptor neuron. The

threshold for a generating action potential was 1–3 pA. Vomeronasal receptor neurons of the frog, turtle and mouse also sensitively responded to current stimulations (Trotier *et al.*, 1993; Taniguchi *et al.*, 1996b; Liman and Corey, 1996). These results indicated that high sensitivity to small depolarizing currents is common to the vomeronasal receptor neurons of these animals.

In the frog vomeronasal receptor neuron, a voltage-dependent Ca^{2+} current was observed in iso-osmotic $BaCl_2$ (Trotier *et al.*, 1993). Ca^{2+} currents, though, were much more easily recorded in the rat vomeronasal receptor neuron; depolarizing voltage pulses induced a voltage-dependent Ca^{2+} current in 10 mM $CaCl_2$ external solution and even in normal Tyrode solution containing 2 mM $CaCl_2$. Intracellular Ca^{2+} plays important roles in olfactory receptor neurons such as activation of phosphodiesterase (Borisy *et al.*, 1992), modulation of adenylyl cyclase (Choi *et al.*, 1992; Frings, 1993) and desensitization of IP_3-induced currents (Kashiwayanagi, 1996). In olfactory neurons, Ca^{2+} also entered through IP_3-gated channels (Kashiwayanagi, 1996). Therefore, Ca^{2+} that entered through a voltage-dependent Ca^{2+} channel together with Ca^{2+} entered through IP_3-gated channels may regulate transduction steps in vomeronasal receptor neurons.

ES20, a chemoattractant extracted from garter snake prey (Jiang *et al.*, 1990), increased IP_3-content in the snake's vomeronasal epithelium (Luo *et al.*, 1994). In the previous study, we found that dialysis of IP_3 into the turtle vomeronasal receptor neurons induced large inward currents (Taniguchi *et al.*, 1995). These results suggest that IP_3 mediates pheromonal information in the reptile vomeronasal organs. In rat vomeronasal receptor neurons, IP_3 also induced excitatory responses, although the amplitude of inward currents induced by 100 μM IP_3 in the rat vomeronasal receptor neuron was relatively small. However, the voltage sensitivity of the rat vomeronasal receptor neuron is very high. Therefore, small inward currents evoked via the IP_3-gated channel should induce the generation of action potentials. Although pheromones, which induce IP_3 accumulation in the rat vomeronasal receptor neuron, have not been found at present, it is likely that pheromonal information is mediated via IP_3-dependent pathways in the rat vomeronasal organ.

In the frog olfactory neuron, dialysis of IP_3 did not induce inward currents in the external solution containing no Na^+ and Ca^{2+} (Kashiwayanagi, 1996). The inward current fluctuations induced by D-IP_3 and L-IP_3 in the rat vomeronasal receptor neuron were also blocked by elimination of Na^+ and Ca^{2+} in the external solution. Ruthenium red has been shown to block IP_3-induced responses in turtle vomeronasal receptor neurons (Taniguchi *et al.*, 1995) and lobster, catfish and rat olfactory neurons (Fadool and Ache, 1992; Miyamoto *et al.*, 1992; Okada *et al.*, 1994). In the rat vomeronasal receptor neuron, the inward current fluctuations induced by D-IP_3 and L-IP_3 were also inhibited by ruthenium red. These results suggested that the IP_3-gated channel in the rat vomeronasal receptor neuron has similar characteristics to those in olfactory neurons.

Stereoselectivity of IP_3 recognition varied among IP_3 binding sites of enzymes and receptors. The IP_3 receptor of bovine adrenal cortex recognize D- and L-isomers with similar affinity (Luong *et al.*, 1991). Both stereoisomers exhibited equipotent affinities for IP_3 phosphatase (Luong *et al.*, 1991) and there was not a remarkable difference in the inhibitory potency of the two stereoisomers on IP_3 phosphatase (Polokoff *et al.*, 1988). However, the L-isomer was less effective in stimulating calcium release and in inhibiting IP_3 kinase (Polokoff *et al.*, 1988). In the rat vomeronasal receptor neuron, amplitude of the inward current and the number of cells showing responses induced by D-IP_3 were similar to those induced by L-IP_3.

ACKNOWLEDGEMENTS

This work was supported by a Grant-in-Aid for Scientific Research from the Ministry of Education, Science and Culture, Japan.

REFERENCES

Barry, P.H. and Lynch, J.W. (1991) Liquid junction potentials and small cell effects in patch-clamp analysis. *J. Membr. Biol.*, **121**, 101–107.

Berghard, A. and Buck, L.B. (1996) Sensory transduction in vomeronasal neurons: evidence for $G_{\alpha o}$, $G_{\alpha i2}$, and adenylyl cyclase II as major components of a pheromone signaling cascade. *J. Neurosci.*, **16**, 909–918.

Berghard, A., Buck, L.B. and Liman, E.R. (1996) Evidence for distinct

signaling mechanisms in two mammalian olfactory sense organs. *Proc. Natl. Acad. Sci. USA*, **93**, 2365–2369.

Borisy, F.F., Ronnett, G.V., Cunningham, A.M., Juilfs, D., Beavo, J. and Snyder, S.H. (1992) Calcium/calmodulin-activated phosphodiesterase expressed in olfactory receptor neurons. *J. Neurosci.*, **12**, 915–923.

Bradley, J., Li, J., Davidson, N., Lester, H.A. and Zinn, K. (1994) Heteromeric olfactory cyclic nucleotide-gated channels: a subunit that confers increased sensitivity to cAMP. *Proc. Natl. Acad. Sci. USA*, **91**, 8890–8894.

Choi, E.-J., Xia, Z. and Storm, D.R. (1992) Stimulation of the type III olfactory adenylyl cyclase by calcium and calmodulin. *Biochemistry*, **31**, 6492–6498

Fadool, D.A. and Ache, B.W. (1992) Plasma membrane inositol 1,4,5-trisphosphate-activated channels mediate signal transduction in lobster olfactory receptor neurons. *Neuron*, **9**, 907–918.

Frings, S. (1993) Protein kinase C sensitizes olfactory adenylate cyclase. *J. Gen. Physiol.*, **101**, 183–205.

Halpern, M. (1987) The organization and function of the vomeronasal system. *Annu. Rev. Neurosci.*, **10**, 325–362.

Halpern, M., Shapiro, L. S. and Jia, C. (1995) Differential localization of G proteins in the opossum vomeronasal system. *Brain Res.*, **677**, 157–161.

Hamill, O.P., Marty, A., Neher, E., Sackmann, B. and Sigworth, E.J. (1981) Improved patch-clamp techniques for high-resolution current recording from cells and cell-free membrane patches. *Pflüger's Arch.*, **391**, 85–100.

Jia, C.P. and Halpern, M. (1996) Subclasses of vomeronasal receptor neurons: Differential expression of G proteins ($G_{i\alpha 2}$ and $G_{o\alpha}$) and segregated projections to the accessory olfactory bulb. *Brain Res.*, **719**, 117–128.

Jiang, X.C., Inouchi, J., Wang, D. and Halpern, M. (1990) Purification and characterization of a chemoattractant from electric shock-induced earthworm secretion, its receptor binding, and signal transduction through the vomeronasal system of garter snakes. *J. Biol. Chem.*, **265**, 8736–8744.

Johns, M.A., Feder, H.H., Komisaruk, B.R. and Mayer, A.D. (1978) Urine-induced reflex ovulation in anovulatory rats may be a vomeronasal effect. *Nature*, **272**, 446–468.

Kashiwayanagi, M. (1996) Dialysis of inositol 1,4,5-trisphosphate induces inward currents and Ca^{2+} uptake in frog olfactory receptor cells. *Biochem. Biophys. Res. Commun.*, **225**, 666–671.

Kashiwayanagi, M. and Kurihara, K. (1995) Odor responses after complete desensitization of the cAMP-dependent pathway in turtle olfactory cells. *Neurosci. Lett.*, **193**, 61–64.

Lepri, J.J., Wysocki, C.J. and Vandenbergh, J.G. (1985) Mouse vomeronasal organ: effects on chemosignal production and maternal behavior. *Physiol. Behav.*, **35**, 809–814.

Liman, E.R. and Buck, L.B. (1994) A second subunit of the olfactory cyclic nucleotide-gated channel confers high sensitivity to cAMP. *Neuron*, **13**, 611–621.

Liman, E.R. and Corey, D.P. (1996) Electrophysiological characterization of chemosensory neurons from the mouse vomeronasal organ. *J. Neurosci.*, **16**, 4625–4637.

Luo, Y., Lu, S., Chen, P., Wang, D. and Halpern, M. (1994) Identification of chemoattractant receptors and G-proteins in the vomeronasal system of garter snakes. *J. Biol. Chem.*, **269**, 16867–16877.

Luong, T.-T., Buylain, B. and Guillemette, G. (1991) Study on the stereoselectivity of inositol 1,4,5-trisphosphate recognition sites of bovine adrenal cortex. *Can. J. Physiol. Pharmacol.*, **70**, 434–441.

Miyamoto, T., Restrepo, D., Cragoe, E.J. and Teeter, J.H. (1992) IP_3- and cAMP-induced responses in isolated olfactory receptor neurons from the channel catfish. *J. Membr. Biol.*, **127**, 173–183.

Okada, Y., Teeter, J.H. and Restrepo, D. (1994) Inositol 1,4,5-trisphosphate-gated conductance in isolated rat olfactory neurons. *J. Neurophysiol.*, **71**, 595–602.

Okamoto, K., Tokumitsu, Y. and Kashiwayanagi, M. (1996) Adenylyl cyclase activity in turtle vomeronasal and olfactory epithelium. *Biochem. Biophys. Res. Commun.*, **220**, 98–101.

Polokoff, M.A., Bencen, G.H., Vacca, J.P., deSolms, S.J., Young, S.D. and Huff, J.R. (1988) Metabolism of synthetic inositol trisphosphate analogs. *J. Biol. Chem.*, **263**, 11922–11927.

Powers, J.B. and Winans, S.S. (1975) Vomeronasal organ: critical role in mediating sexual behavior of the male hamster. *Science*, **187**, 961–963.

Rajendra, S., Lynch, J.W. and Barry, P.H. (1992) An analysis of Na^+ currents in rat olfactory receptor neurons. *Pflüger's Arch.*, **420**, 342–346.

Rajendren, G. and Dominic, C.J. (1985) Effect of bilateral transection of the lateral olfactory tract on the male-induced implantation failure (the Bruce effect) in mice. *Physiol. Behav.*, **36**, 587–590.

Sipos, M.L., Wysocki, C.J., Nyby, J.G., Wysocki, L. and Nemura, T.A. (1995) An ephemeral pheromone of female house mice: perception via the main and accessory olfactory systems. *Physiol. Behav.*, **58**, 529–534.

Taniguchi, M., Kanaki, K. and Kashiwayanagi, M. (1996a) Difference in behavior between responses to forskolin and

general odorants in turtle vomeronasal organ. *Chem. Senses*, **21**, 763–777.

Taniguchi, M., Kashiwayanagi, M. and Kurihara, K. (1996b) Intracellular dialysis of cyclic nucleotides induces inward currents in turtle vomeronasal receptor neurons. *J. Neurosci.*, **16**, 1239–1246.

Taniguchi, M., Kashiwayanagi, M. and Kurihara, K. (1995) Intracellular injection of inositol 1,4,5-trisphosphate increases a conductance in membranes of turtle vomeronasal receptor neurons in the slice preparation. *Neurosci. Lett.*, **188**, 5–8.

Trotier, D., Døving, K.B. and Rosin, J.F. (1993) Voltage-dependent currents in microvillar receptor cells of the frog vomeronasal organ. *Eur. J. Neurosci.*, **5**, 995–1002.

Wysocki, C.J. and Meredith, M. (1987) The vomeronasal system. In Finger, T.E. and Silver, W.L. (eds), *Neurobiology of Taste and Smell*. Wiley, New York, pp. 125–150.

Wysocki, C.J., Wellington, J.L. and Beauchamp, G.K. (1980) Access of urinary nonvolatiles to the mammalian vomeronasal organ. *Science*, **207**, 781–783.

Received October 20, 1996; accepted November 8, 1996